Percolating Transport and the Conductive Scaling Relationship in Lamellar Block Copolymers under Confinement

Kyle M. Diederichsen, Ryan R. Brow, and Mark P. Stoykovich*

Department of Chemical and Biological Engineering, University of Colorado Boulder, Boulder, Colorado 80309, United States

ABSTRACT The topology and transport behavior of the lamellar morphology self-assembled by block copolymers in thin films are shown to depend on the length scale over which they are characterized and can be described by percolation in a network under confinement. Gold nanowires replicating the lamellar morphology were fabricated *via* self-assembled poly(styrene-*block*-methyl methacrylate) thin films and a lift-off pattern transfer process. The lamellar morphology exhibits long-range connectivity (macroscopic scale); however, characterization of electrical conduction over confined areas (5−500 μm) demonstrates a discrete probability of disconnection that arises due to the underlying network structure and a lack of self-similarity at these microscale dimensions. In particular, it is proved that the lamellar network morphology under confinement has a conductance that is nonlinear with channel length or width. The experimental results are discussed in terms of percolation theory, and a simple, two-dimensional Monte Carlo model is shown to predict the key trends in the network topology and conductance in lamellar block copolymers, including the dependencies on composition, extent of spatial confinement, and confinement geometry. These results highlight the need to exquisitely control or engineer the self-assembled nanostructured pathways formed by block copolymers to ensure consistent device performance for any application that depends upon percolating material, ionic, or electrical transport, especially when confined in any dimension. It is also concluded that the two most promising approaches for enhancing conductivity in block copolymer materials may be achieved either at the limits of (1) perfectly oriented, single-crystalline or (2) high defect density, polycrystalline microphase separated morphologies and that nanostructured systems with intermediate defect densities would be detrimental to transport in confined systems.

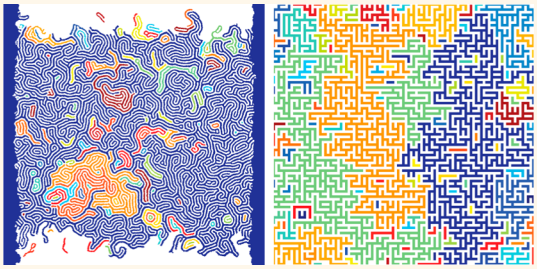

KEYWORDS: block copolymers · lamellae · percolation · transport · topology · network structure · thin film

Block copolymers self-assemble into a variety of nanoscale morphologies[1] that have been exploited in two or three dimensions for applications ranging from lithographic templates[2−6] to membranes and nanoporous materials.[7−11] The transport behavior of small molecules, ions, protons, or electrons through the nanostructured materials is often an important consideration for final device performance, for example, in organic photovoltaics,[12,13] solid electrolytes for batteries and energy storage devices,[14,15] or nanofiltration membranes.[16,17] Although bicontinuous morphologies such as the gyroid or those formed by triblock copolymers provide multiple transport pathways and can simultaneously maintain the structural/mechanical integrity of the material,[18−20] cylindrical and lamellar structures have attracted much interest due to their processability in either the bulk or films and an extensive understanding of these morphologies across scales (from the molecular level to the domain correlation length to the grain scale and beyond). The overall transport behavior in cylindrical and lamellar morphologies, however, is anisotropic and dictated, in part, by a finite domain grain size and the nature of the defects that constitute the grain boundaries. Furthermore, transport may be enhanced in such systems by domain alignment techniques (*e.g.*, magnetic fields,[21] electric fields,[22] or shear[23]) to achieve more direct pathways. Specific transport pathways can be difficult to elucidate in the three-dimensional systems that have been considered, and rather, the

* Address correspondence to mark.stoykovich@colorado.edu.

Received for review July 31, 2014 and accepted March 10, 2015.

Published online March 10, 2015
10.1021/acsnano.5b01321

average transport properties of the material are characterized in combination with techniques such as scattering that provide information on average structure.[24,25]

Thin films present an opportunity to directly study the domain interconnectivity (*i.e.*, the network topology) present in self-assembled block copolymer systems because the generated morphology is easily imaged through top-down characterization techniques such as scanning electron microscopy (SEM) or atomic force microscopy (AFM). Network topology, in block copolymer systems, may be defined as the spatial arrangement and interconnectedness of the domains (*i.e.*, links) and defects (*i.e.*, nodes) that define the long-range structure of the morphology. Using such an approach in lamellae self-assembled by poly(styrene-*block*-methyl methacrylate) (PS-*b*-PMMA) in thin films, we have previously quantified the areal density of branch points and end points, as defined by dislocation and disclination type defects, to understand the local connectivity of the network elements and the corresponding impact of the defect population on the long-range percolation of the network.[26] The presence of many nodes in the network favors the self-assembly of an interconnected network and a high degree of redundancy of percolating pathways. Therefore, continuous, percolating networks are generated in the domain with the greatest volume fraction, such that slightly asymmetric but lamellar-forming PS-*b*-PMMA block copolymers with a PMMA volume fraction of $f_{PMMA} = 0.45$ or 0.55 form percolating networks over infinite areas in the PS or PMMA domains, respectively.[26,27]

Here the impact of confinement on conductive transport in two-dimensional lamellar nanostructures self-assembled by block copolymers in thin films is explored in terms of percolating random networks. Specifically in this work, the conductance in the networks formed by PS-*b*-PMMA in thin films has been characterized over distances of 5 to 500 μm by replication of the lamellar pattern into metal nanowires and is demonstrated to have a strong dimensional dependence as a result of spatial confinement of the underlying network structure. The lamellar structure is shown to be analogous to a random network that is well described by percolation theory, independent of thermodynamic considerations. Percolation theory, in conjunction with effective medium theory, has been applied previously to describe transport in polymer blends by Ottino and Sax,[28,29] demonstrating a threshold for network percolation as a function of volume fraction and non-Fickian diffusion entirely as a result of system morphology. Later the theory was extended to copolymer membranes, and scaling factors for transport were defined that were dependent on the microscale morphology.[30] It has since been shown that finite size effects introduced by grain boundaries limit the applicability of the percolation theory treatment,[31,32] although the power law scaling of conductivity as a function of volume fraction has been shown in a number of copolymer membranes.[33,34] In this article, we demonstrate that percolation theory can describe many of the topological and transport features of networks self-assembled by lamellar block copolymers in thin films and that conductance in these confined networks is nonlinearly dependent on dimension. The importance of confinement in block copolymer systems is broadly important for any application that depends on domain connectivity, and the results herein suggest the need for one of two limiting self-assembled morphologies to achieve favorable transport properties and consistent device performance: either perfectly aligned and oriented domains (*i.e.*, single-crystalline) as through directed self-assembly or highly interconnected, high defect density (*i.e.*, polycrystalline) morphologies.

RESULTS AND DISCUSSION

Electrical conduction measurements were chosen here to characterize the transport behavior within block copolymer structures, primarily because of the well-established and readily available tools for performing such measurements at the nano- and microscales. Facile characterization of the self-assembled block copolymer thin film morphology was therefore achieved by replicating, using lithographic and pattern transfer processes, the lamellar structures into metal nanowire networks, which were then electrically probed and directly imaged in real space. Figure 1A highlights the lift-off based strategy used to fabricate the metal nanowire networks in the pattern of self-assembled block copolymer lamellae.[3,35−37] PS-*b*-PMMA thin films ($\bar{M}_n \approx 100$ kg mol^{-1} with tunable volume fraction f_{PMMA}; film thicknesses of ~45 nm) were self-assembled *via* thermal annealing on neutral PS-r-PMMA brush layers[38,39] on an electrically insulating SiO_2 substrate to produce perpendicular lamellae with a periodicity of $L_o \approx 50$ nm. The PMMA domain was then selectively removed *via* exposure to UV light, an acetic acid rinse, and a short O_2 plasma reactive ion etch. The remaining PS template was used as a mask for the deposition of 15 nm gold (Au) films by thermal evaporation. Networks of Au nanowires were then fabricated across the substrate by lifting-off the PS template by sonicating overnight in toluene. The confined nanowire networks were examined by SEM and found to replicate with fidelity the PMMA domain of the block copolymer structures. Higher resolution images, including before and after pattern transfer, of the Au nanowires can be found in the Supporting Information (Figure S1).

Channels of varying width ($W = 5$ or 20 μm) were lithographically defined in the nanowire network, and

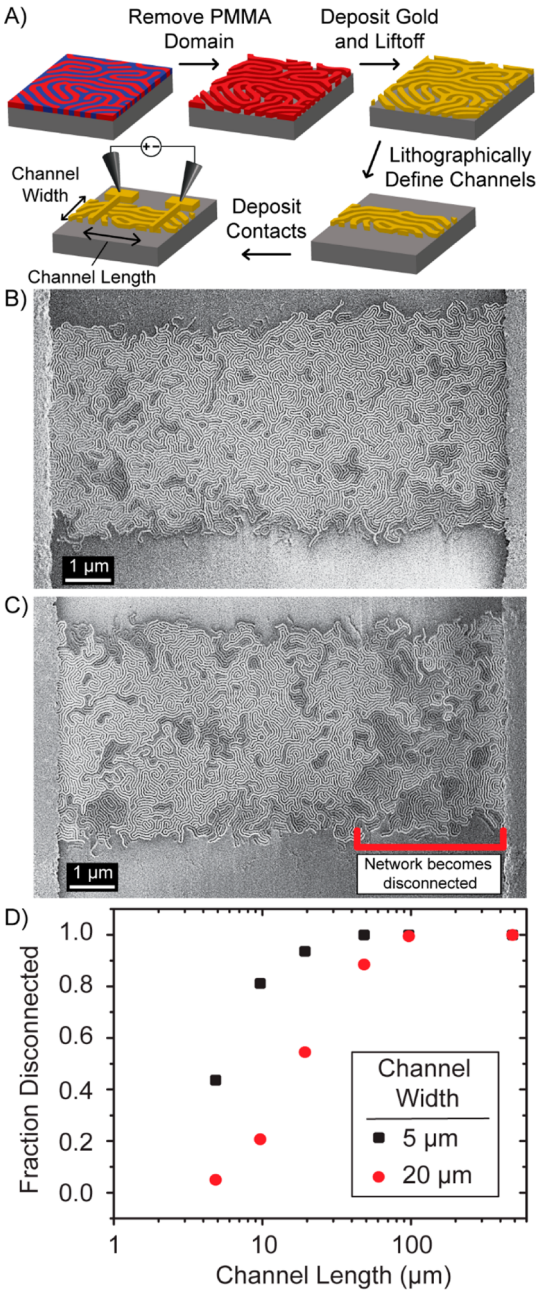

Figure 1. Characterization of percolation in Au nanowire networks defined by lamellar-forming PS-*b*-PMMA with f_{PMMA} = 0.52. (A) Schematic of the fabrication process for confined nanowire networks in the structure of lamellar block copolymer thin films. (B) Scanning electron micrograph of a connected pair of contacts (50 nm thick Au contacts can be seen on the left and right edges of the image) with a 10 μm channel length and a 5 μm channel width. The nanowire network appears bright when connected over large areas. (C) SEM image of a disconnected pair of contacts for a channel of 10 μm in length and 5 μm in width. The left side of the network does not connect to the right, resulting in the contacts displaying a different brightness. (D) Fraction of networks that were disconnected or nonpercolating as a function of channel length for channel widths of 5 and 20 μm, as characterized by electrical conductance measurements.

contacts were deposited with varied spacing to yield channel lengths (*L*) from 5 to 500 μm on the same sample. Connectivity between neighboring contacts was then investigated, as shown in Figure 1B and C for a 5 μm $\times$ 10 μm channel (higher resolution versions available as Figure S2 in the Supporting Information). On insulating substrates such as SiO_2, isolated Au nanowire elements become charged in the SEM and, as such, appear darker than networks that percolate over large areas and that can conduct charge away from the imaged area. In Figure 1B, the nanowire network appears to have approximately the same brightness between the contacts (shown on the left and right sides of the image), indicative of an electrical connection between the contacts, though some isolated elements are contained within the channel. Figure 1C demonstrates a channel where the left portion of the network does not connect to the right contact, as indicated by the darker nanowire regions that span the entire channel width from the top to the bottom.

Electrical current−voltage (*IV*) characterization was performed by application of a small voltage bias to the contacts and was used to rapidly verify the availability of transport pathways and network percolation. The fraction of disconnected contacts is shown in Figure 1D and was determined by characterizing over 75−210 distinct channels of each dimension. Increasing the channel length between neighboring contacts resulted in a larger fraction of disconnected contacts, while increasing the channel width decreased the fraction of disconnected contacts. The localized connectivity of the networks produced by block copolymer thin films is highly dependent on the length scale over which it is measured, despite the fact that this block copolymer, when unconfined, has a composition exceeding the critical threshold necessary for substrate-spanning percolation.[26]

By close examination of the network structure, it is clear that the disconnected networks arise as a result of the limited number of pathways between contacts. Figure 2A displays a representative network in a 5 μm $\times$ 5 μm channel. Connectivity of this network can be investigated by a simple image analysis, as shown in Figure 2B, in which domains belonging to a continuous, interconnected network are assigned the same color. The region contains a large percolating network, colorized in dark blue, but it also contains a number of small disconnected areas. Image analysis of the nanowire network furthermore allows full simulation of the electrical circuit in NGSpice,[40] assuming each nanowire is a constant size (15 nm tall $\times$ 25 nm wide) and that the electrical resistivity of Au at this size scale on SiO_2 is 6.5×10^{-8} $\Omega \cdot$m.[41] This calculation yields a current map of the nanowire network (Figure 2C), in which segments that carry the most current are colorized in bright red.

The comparison of Figure 2B and C clearly demonstrates that, although the percolating network fills the

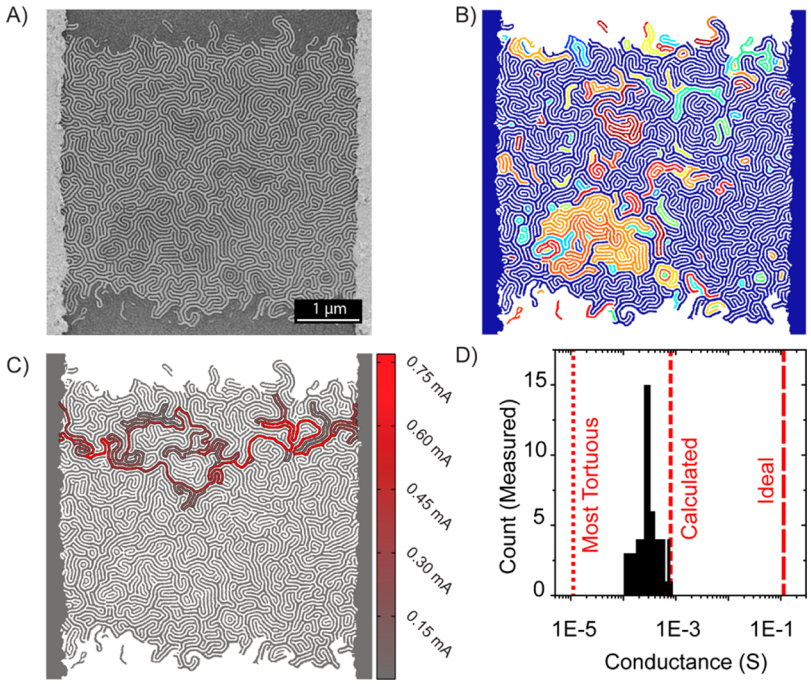

Figure 2. Conductance in Au nanowire networks defined by lamellar-forming PS-*b*-PMMA with $f_{PMMA} = 0.52$. (A) SEM image of a 5 μm $\times$ 5 μm channel that is connected. (B) Network analysis of the SEM image in (A) in which connected and continuous nanowire elements are assigned the same color. (C) Calculated current map of the nanowire channel with a 1 V potential applied across the contacts. Only a small fraction of the nanowires contribute to conductance. (D) Histogram of measured conductances for channels 5 μm $\times$ 5 μm in size, with the most tortuous, ideal, and calculated conductance for the current map in (C) overlaid.

majority of the confined area, the left to right connectivity of the nanowire channel is reliant on only a single critical pathway, which, if broken, causes the channel to become completely disconnected. As such, it becomes clear how confinement may prohibit electrical transport between contacts even when the network is connected over infinitely large areas. Along any individual path in the nanowire network, there are critical nodes that must be connected to provide for percolating transport. If any one of these nodes is not connected, the network loses an entire pathway across the substrate, and thus, if enough nodes are removed, the network would no longer be percolating. Confinement increases the likelihood that critical nodes will be excluded from the network and that network percolation will be lost. For narrow channels (small W), there will be fewer percolating pathways and, as such, it is more probable for a critical node to be lost and the network to become disconnected. For long channels (large L), pathways must persist in a single direction for a greater distance, thereby increasing the number of nodes along a single path that must be connected in series and the likelihood that a path will be disconnected.

The calculation of the current map and channel conductance may be compared to the empirically measured results for this channel size and the two theoretical extremes for conductance. At one extreme, the most tortuous and lowest conductance pathway through the channel would be a serpentine path that occupies the entire area, but only contains a single pathway (*i.e.*, 1 path of length $\approx W(L/L_0) + L$, where L_0 is the lamellar periodicity). The theoretical case with the highest conductance, on the other extreme, is that of many straight connecting paths between the two contacts that are in parallel (*i.e.*, W/L_0 paths of length L). Figure 2D displays a histogram of the conductance measured for 85 distinct 5 μm $\times$ 5 μm channels overlaid with the theoretical predictions for the most direct and most tortuous paths. Note that these data exclude disconnected channels. The calculated conductance for the network in Figure 2A–C of 8.04×10^{-4} S lies toward the upper end of the measured distribution, but is reasonable given that the real Au nanowires may have a conductivity slightly lower than that assumed from the literature (*e.g.*, perhaps due to differences in nanowire surface roughness or Au density that arise in the metal deposition technique).

A Monte Carlo model of random percolating networks was used to provide insight into the connectedness and conductance of block copolymer lamellae in thin films, specifically to consider the effect of the extent of confinement and network topology as controlled through the domain concentration. This bond percolation model is based on the square lattice shown in Figure 3A (panel 1), with periodic boundary conditions applied in both directions. In panels 2 and 3, connections between adjacent nodes are filled

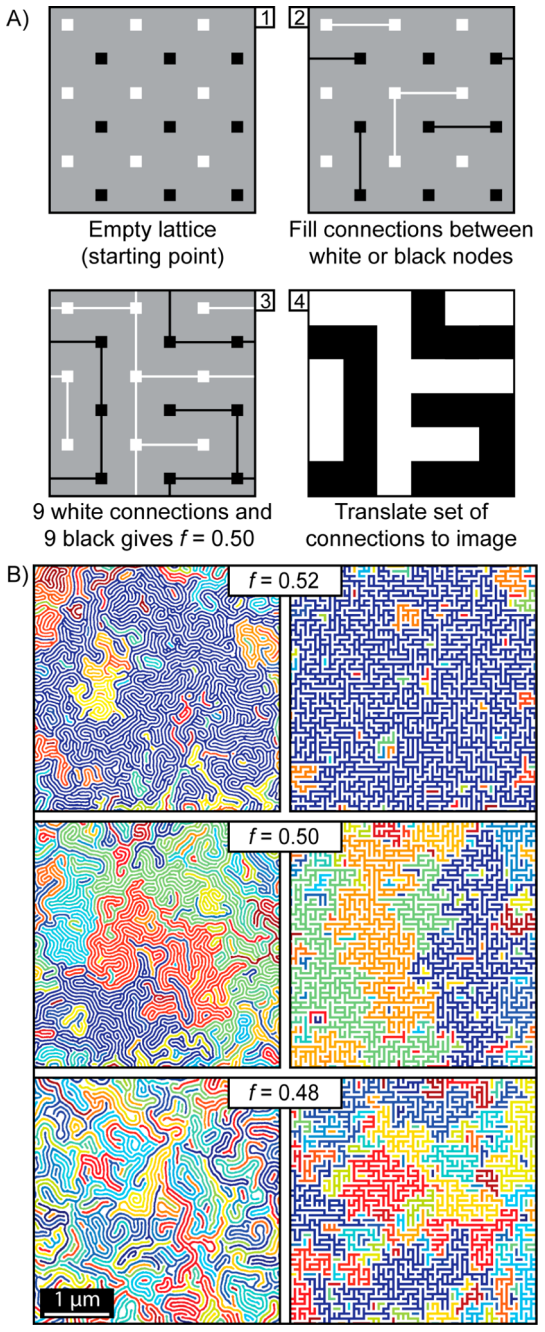

Figure 3. (A) Illustration of the key steps (panels 1−4) in the Monte Carlo bond percolation model. A lattice of black and white nodes (example 3 × 3 lattice is shown) is filled with connections to meet a specified volume fraction of the white domain, including periodic boundary conditions. The model is translated to a black and white image for visualization and network analysis. (B) Volume fraction (*f*) dependence of the connectivity in the PMMA domain (darker domains in SEM images) for the experimental PS-*b*-PMMA system (left) and black domain for the percolation model (right). Connected and continuous elements in the network are assigned the same color. The model images are analyzed without periodic boundary conditions to match the SEM images of the lamellar block copolymer nanostructures.

randomly to match a specified fraction of white bonds, which is equivalent to the volume fraction or concentration of a block in the copolymer. To provide a link to the physical lamellar morphology, network connections of defects not observed in the block copolymer systems are eliminated by randomly moving bonds that violate these rules to elsewhere in the lattice. Specifically, 4-fold-connected nodes, in which a single node radiates four separate bonds, are forbidden such that the maximum number of connections at any node is specified to be three. Additionally, nodes that are unconnected (*i.e.*, have no bonds) are prohibited because, assuming the nodes themselves do not have any volume, this physically represents a region with nonalternating domains and is inherently not lamellar. No other physical or thermodynamic features of the block copolymer system were included in the percolation model. The modeled set of connections is translated to a black and white image (Figure 3A, panel 4), which can then be analyzed for domain connectivity and resistance in the same manner as SEM images of the block copolymer morphology or the nanowire domains (as in Figure 2B and C).

Figure 3B visually illustrates one of the key trends in block copolymer systems replicated by the model. It has been shown previously that the defect population and consequently the network morphology of lamellar PS-*b*-PMMA thin films is a function of the relative volume fraction of each block (discussed throughout this article in terms of the PMMA component, f_{PMMA}).[26] In particular, decreasing the volume fraction of PMMA from above the symmetry point (*e.g.*, $f_{PMMA} = 0.52$) to below the symmetry point (*e.g.*, $f_{PMMA} = 0.48$), as in the colorized SEM images of PS-*b*-PMMA lamellae in the left column of Figure 3B, causes the density of defects that serve as branches to decrease relative to those that serve as end points. Correspondingly the network in the PMMA domain becomes less interconnected and fails to percolate over the imaged area. Despite the lack of thermodynamic considerations, simulations of the percolation model yield structures that accurately reproduce this key trend in lamellar network connectivity. Network analysis of the black domain, as shown in the colorized images in the right column of Figure 3B for $f_{black} = 0.52$ to 0.48, displays a transition from a percolating network to a disconnected structure. In both the block copolymer system and the percolation model, the complementary domains (*i.e.*, the PS or white domains) mirror the trend presented here, such that increasing the volume fraction of either domain leads to increased connectivity of that domain.

The transition in connectivity is well described by percolation theory in terms of the critical threshold probability of having a bond between nodes (f_c). This probability is analogous to the symmetric volume fraction in real copolymer systems. For an infinitely large lattice, the critical threshold indicates the probability above which a percolating network that spans the entire area (an "infinite network") exists with certainty and below which no such network is possible. For a square

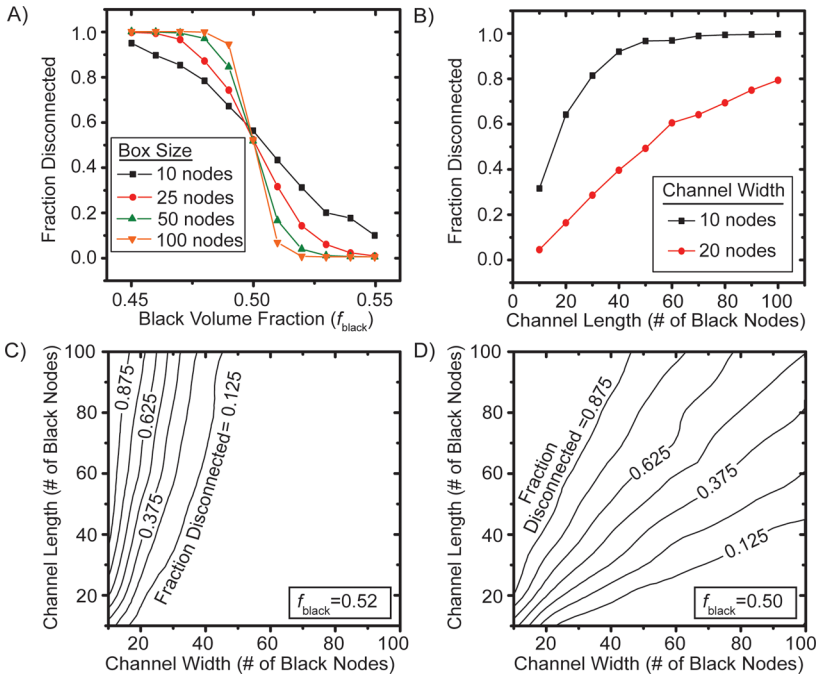

Figure 4. (A) Fraction of disconnected or nonpercolating networks in the black domain as a function of the black concentration (f_{black}) for model square boxes of different size (a square number of nodes such that $L = W$). The connectivity of the white domain with respect to the white concentration follows the same trend. (B) Fraction of disconnected networks in the black domain of the modeled network as a function of the channel length for two different channel widths at a volume fraction of $f_{black} = 0.52$. Contour maps of the fraction of disconnected networks (with connectivity measured in the direction of channel length) as a function of channel width and length for a black volume fraction of (C) $f_{black} = 0.52$ and (D) $f_{black} = 0.50$. Each data point presented represents the average of 1000 distinct simulated networks.

lattice in the Monte Carlo bond percolation model, without additional rules, this transition has been solved analytically to have a critical point at $f_c = 0.5$.[42] The exact critical percolation threshold for the model used here is less obvious, but may be anticipated to be similar to this value. It is known that decreasing the coordination number of the nodes in the lattice causes the critical percolation threshold to increase due to fewer possible paths leading away from any node.[29] By similar logic, limiting the number of bonds at any node to three should increase the critical fraction for the percolation transition, although also imposing a minimum of one bond per node is likely to offset this increase. This critical threshold probability is analogous to the symmetric volume fraction in real copolymer systems. For the PS-*b*-PMMA system, the symmetry point of the phase diagram (*i.e.*, the point of zero spontaneous curvature) is near $f_{c,PMMA} = 0.51$, which matches well with the actual observed transition in Figure 3B.[26,43] Although other block copolymer systems have different symmetry points dependent upon the statistical segment lengths of the components,[44,45] the key trends described here are generally applicable. A straightforward Monte Carlo model may be able to accurately describe any copolymer system if the lattice and bonding rules are given careful consideration, as the critical threshold is dependent on this choice.

When a network is confined, as is the case for any real block copolymer system, the transition between a percolating and nonpercolating structure (a connected *versus* disconnected system, respectively) is no longer a step function at f_c. Instead, broad transitions between connected and disconnected networks are calculated using the Monte Carlo (MC) simulations as shown in Figure 4A. Over a thousand repeats, for a large box size (with $W = L$ as specified by the number of lattice points) the network has a relatively sharp transition, but the transition broadens considerably with decreasing box size. Experimental measurements taken at $f_{PMMA} = 0.52$ (Figure 1D), which is close to, but above, the critical transition that is predicted near $f_{c,PMMA} = 0.51$ for the block copolymer system, lie within the broadened transition region caused by system confinement and exhibit some probability of disconnection. Systems with domain concentrations further away from the critical point diminish the impact of confinement due to the change in the defect population, with more interconnecting branch points above $f_{c,PMMA}$ and more end points below $f_{c,PMMA}$. Regardless, because real networks are never infinite, there is always some discrete probability of disconnection above the critical threshold and connection below it. A second set of *IV* measurements attempted on ~250 nanowire networks fabricated by a PS-*b*-PMMA block copolymer with $f_{PMMA} = 0.48$ did not show any indication of connection at any of the channel dimensions that were probed ($W = 20\,\mu$m and $L = 5$ to $500\,\mu$m). While channel lengths small enough (or channel widths large

enough) to yield a percolating connection in the $f_{PMMA} = 0.48$ system are predicted to exist, lithographic limitations did not allow their fabrication and characterization here.

Figure 4A considers percolation over the area of the simulated box in both the top-to-bottom and left-to-right directions, whereas the experiments reported in Figure 1D probed conductance in only one direction. Shown in Figure 4B, the MC percolation model was thus applied to one-dimensional percolation for a bond composition of $f_{black} = 0.52$ and 1000 repeats. The appearance of a percolating system is found to be strongly dependent on the dimensions to which the network is confined. The close agreement of the trend predicted by the percolation model to the experimental observation supports a conclusion that two-dimensional lamellar block copolymers in thin films are effectively random percolating networks and follow the predictions of percolation theory. It should be noted that if the length scale of the modeled domains is matched directly to the size of the real block copolymer domains, 25 nm wide, the effects of confinement on percolation theory are observed at smaller dimensions than in the real system. As a result, a quantitative match between the model and experiments is not appropriate here because the model does not effectively define length scales and generates a much higher defectivity (*i.e.*, the number of branch and end points per unit area) than a block copolymer system with thermodynamic considerations that lead to defect annihilation in an attempt to minimize the free energy of the overall system.

The percolation model can be extended to describe network connectivity for a wide range of channel geometries and bond concentrations. In Figure 4C and D, contour plots for the probability of disconnection as a function of channel width and length are shown for compositions above and near the critical point of the system, respectively. Above the critical point f_c, it is clear that there is a strong dependence on channel width such that wide channels always provide percolating pathways. In a system with a volume fraction of $f_{black} = 0.50$ (Figure 4D), there is an almost equivalent dependence on both channel length and width because the system is more likely to be disconnected at any length scale and the dimension of confinement becomes less important. It can be seen that, in either case, the limit of infinite channel width relative to channel length will always yield percolating connectivity regardless of the channel length. The opposite is true as well: connectivity is never achieved in the limit of infinite channel length relative to channel width.

The channel length dependence of conductance measured in the nanowire networks defined by PS-*b*-PMMA with $f_{PMMA} = 0.52$ is plotted in Figure 5A. A power law scaling with an exponent of -1.2 to -1.3 is found, thus indicating a nonlinear length dependence. Error bars on this plot indicate one standard deviation from the mean. Analysis of the full data set indicates that these exponents statistically differ from the linear case with 95% and 90% confidence for the 20 and 5 μm wide channels, respectively. As further verification of the nonlinearity of confined networks, the conductance of the Monte Carlo simulated networks was analyzed by assigning a conductivity and length scale to the bonds. A circuit analysis of the simulated networks was then performed using the NGSpice

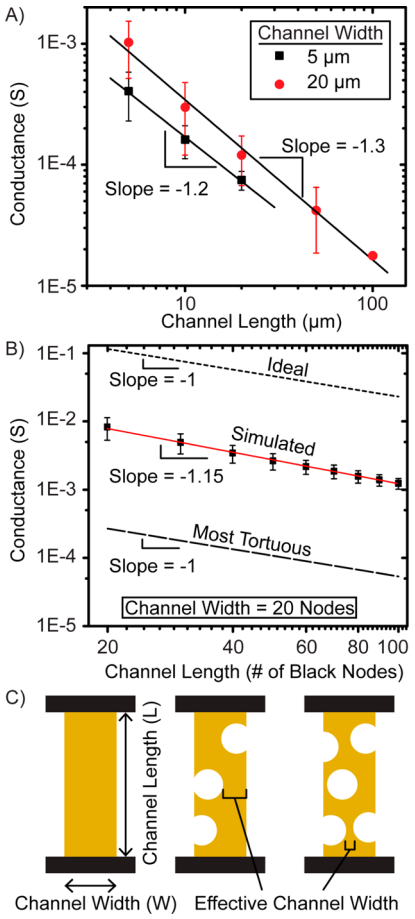

Figure 5. (A) Conductance of the Au nanowire networks from lamellar-forming PS-*b*-PMMA with $f_{PMMA} = 0.52$ as a function of channel length for channel widths of $W = 5$ and 20 μm. The slope of the fit lines yields scaling exponents of -1.2 and -1.3 for the $W = 5$ and 20 μm channels, respectively. Error bars represent one standard deviation of the measured value. Note that the final data point for the 20 μm line does not have an error bar, as only one connected pair of contacts was found in the 210 contacts that were fabricated. (B) Average conductance of the simulated Monte Carlo model as a function of channel length for a channel width of 20 nodes and 1000 repeats. The slope of the fit line yields a scaling exponent of -1.15. Error bars represent one standard deviation of the calculated value. The conductance of the ideal and most tortuous possible pathways are an order of magnitude higher and lower, respectively, than the simulated system and both scale linearly. (C) Illustration of the effective channel width between two contacts (shown in black). Removing nonpercolating portions of the network results in a smaller effective channel width available for transport than the as-fabricated channel width.

program. As shown in Figure 5B, the Monte Carlo model also demonstrates power law scaling with an exponent of −1.15, differing from −1 with a confidence level of 99%. Figure 5B also demonstrates the linearity of the most tortuous and direct path cases previously discussed as a function of channel width. On the log scale, the simulated results lie approximately halfway between these cases, similar to the measured system in Figure 2D. As previously mentioned, a direct comparison of the channel widths and lengths between the simulated and real systems is not appropriate because the Monte Carlo model generates networks with much shorter domain persistence lengths and higher defect densities than in block copolymer lamellae.

If the nanowire network in a channel is considered to have homogeneous material properties as in a Au sheet, conductance would scale with L^{-1} and W^{+1}. However, limiting the number of pathways through the channel causes the behavior of the network to diverge from this continuum description. As illustrated in Figure 5C (left), there is a constant length and width for a continuous channel. When sections of the sheet are removed, as a result of lamellar regions that are not connected to the main percolating network or are dangling elements that do not participate in transport, the effective channel width available for conduction is narrower than W (as clearly illustrated in the conductance map of Figure 2C). This concept has been considered theoretically in describing the nonlinearity of conductance in confined random resistor networks and is discussed further in the Supporting Information. The effective path length between contacts is also extended, as there is not a direct transport pathway down the channel. Moreover, as the channel length increases, the probability of the channel width becoming more constricted increases. Therefore, due to the random nature of the self-assembled lamellar network, neither the effective width nor length of the conducting pathways through the channels is actually known. Qualitatively, then, it is reasonable that the block copolymer system displays a more complex scaling behavior with the defined channel length L and channel width W.

This discussion of channel conductivity and effective path length may be considered in terms of a tortuosity factor, where the actual path length through some media is longer than the direct path case. For the networks self-assembled by lamellar block copolymers, the tortuosity is related to the winding pathways through the channel and a concomitant reduction in the number of parallel pathways available for transport. In three-dimensional systems it has been noted that for a random assortment of aligned grains, conductivity will be 2/3 of the perfectly aligned system because, on average, there will be 1/3 of the grains oriented in a direction that does not allow transport through the membrane.[29,31,46] When the two-dimensional system is considered, it may be expected that this factor should be 1/2, as in general pathways can be oriented either in the direction of conduction or normal to that direction. However, as demonstrated in this work, the conductance of the nanowire channel in two dimensions is lower by an order of magnitude than the ideal, aligned path case. Confinement is the major factor here, because the argument for a factor of 1/2 or 2/3 assumes that there are a large number (effectively it requires an infinite number) of individual grains to allow an overall average directionality to be assumed.[31] Additionally the lamellar thin film block copolymer system consists of many tortuous pathways and does not have true grain boundaries, thereby lacking distinct regions of aligned domains. It is reasonable then that the network conductance observed here for two-dimensional networks formed by lamellar block copolymers in thin films is a complex function of the system size and that a simple Monte Carlo model of percolation, with similar structural characteristics, provides important insight into the transport behavior in such materials.

CONCLUSIONS

The experiments and theory presented here demonstrate that confinement of lamellar nanostructures formed by PS-*b*-PMMA in thin films results in a finite probability of local disconnection in the confined regions, despite such nanostructures forming networks that exhibit long-range connectivity and percolation when unconfined. A Monte Carlo model implementing bond percolation theory has been shown to effectively describe the transport behavior in the block copolymer system and captures the transition from percolating to nonpercolating networks as a complex function of both domain volume fraction and length scale. In addition, the conductance of the fabricated nanowire channels and simulated networks has been shown to have a superlinear dependence on the channel length as a result of the underlying random network structure. These results indicate that the application of nanostructures templated by the self-assembly of lamellar block copolymer materials, for example as interconnects or transparent conducting electrodes, must carefully consider the electrical properties of the nanowire network with respect to the device dimensions.

More broadly, these considerations of the nanostructure network topology apply to any block copolymer system that requires domain connectivity and percolating transport, including in three-dimensional geometries. The effects of confinement in such systems may be less pronounced as a result of the additional pathways available in the third dimension,[29] but the same observations are to be anticipated. In the case of a thin membrane with flux orthogonal to its

surface, conducting pathways would be expected for block copolymers with a wide range of domain volume fractions, as the system is analogous to the channels of small length and large width analyzed here. Nevertheless, the random network structure does not guarantee a homogeneous distribution of these pathways throughout the membrane, with entire sections likely being disconnected as a result of the underlying morphology. These disconnected regions will consume a greater fraction of the membrane with increasing membrane thickness and may lead to a nonlinear dependence of the membrane flux similar to that measured here for the two-dimensional nanowire networks (Flux $\approx t^{-\alpha}$ where $\alpha > 1$).

Block copolymer systems in three dimensions, however, have domain correlation lengths and grain sizes that are often larger than in comparable block copolymer systems in thin films,[31,46] which may lead to confinement effects being significant at larger dimensions. Interestingly and in support of such conclusions, Balsara and co-workers recently have shown that ionic conductivity in thick films of a lamellar-forming poly(styrene-*block*-ethylene oxide) system decreased by ~5-fold when the domain grain size increased from 13 nm to 88 nm.[46] Effectively what occurs is that the larger grains limit the total number of percolating pathways that are available for transport through a film of finite thickness. Although the system studied in our work lacks well-defined grains, an analogy can be drawn between the correlation length of the lamellar domains and grain size. Grains are typically defined by defects at their boundary that cause interconnection between domains with different directors; in the lamellar block copolymer system in two dimensions, the correlation length of a domain captures a similar effect by roughly indicating the distance before the domain may encounter a branch or end point. By this analogy, it can be predicted that larger grains would cause the effects of confinement to become more important, in the same way that the system modeled here demonstrates percolation at a smaller length scale than the real lamellar system with longer domain persistence and correlation lengths.

Two attractive approaches to percolating systems are then suggested, either by (1) directed self-assembly to achieve single-crystalline and anisotropic, oriented domains to entirely avoid the issues inherent to random networks or (2) material engineering to produce an isotropic morphology with a small grain size achieved through high defect densities and a predominance of interconnected/branching defects, for example by using more asymmetric lamellar systems far from f_c. Intermediate situations, which might arise due to defect annihilation during annealing or in directed self-assembly techniques that fail to yield single-crystalline systems but substantially increase the grain size, are expected to lead to hindered transport, especially when used in confined geometries. These predictions are consistent with our observation that the key parameter in determining the effect of confinement on percolation is the spacing of the critical network nodes relative to the spatial confinement dimension. In order to achieve the highest conductivity and the greatest number of percolating pathways, it thus would be desirable to minimize the effects of confinement by reducing the spacing between network nodes. Finally, it may be concluded that approaches for defect engineering during self-assembly should provide opportunities to control the network topology and the desired percolating transport behavior in the block copolymer morphologies. The goal of such defect engineering should be to modify the defect population, in terms of the defect density and the relative distribution of the types of defects, through careful selection of materials (*e.g.*, copolymer composition or homopolymer blending to stabilize defects)[47] or processing conditions (*e.g.*, solvent *versus* thermal annealing, annealing temperature, or film thickness).[43,48]

METHODS

Block Copolymer Processing. Silicon (Si(100)) wafers with 1000 nm of thermally grown oxide were purchased from University Wafer. A neutral surface treatment was applied to obtain lamellar poly(styrene-*block*-methyl methacrylate) networks with the domains oriented perpendicular to the substrate.[49,50] The oxide surface was cleaned *via* submersion in a piranha solution of 70% sulfuric acid and 30% hydrogen peroxide at 70 °C for 30 min and then sequentially rinsed in water, acetone, and toluene. A random copolymer with a molar composition of 58% styrene, 31% methyl methacrylate, and 2% glycidyl methacrylate was spin-cast at 4000 rpm on the dried substrates from a 0.3 wt % solution in anhydrous toluene. This film was then thermally treated at 190 °C for 2 h to produce a cross-linked mat. Sonication in toluene following annealing removed any unreacted polymer and provided a neutral surface for block copolymer self-assembly.

Poly(styrene-*block*-methyl methacrylate) (PS-*b*-PMMA) with total molecular weights $\bar{M}_n$ = 105, 101, and 107 kg mol^{-1} (PDI = 1.09, 1.12, and 1.16, respectively) and PMMA volume fractions of f_{PMMA} = 0.52, 0.50, and 0.48, respectively, were purchased from Polymer Source, Inc. A solution of 1.5 wt % polymer in anhydrous toluene was prepared by dropwise addition to the dry polymer, and ~45 nm thin films were spin-cast at 4000 rpm onto the prepared neutral substrates. The films were then annealed at 210 °C for 24 h under ~10 Torr vacuum to allow for self-assembly.

Fabrication of Gold Nanowires. The self-assembled block copolymer nanostructures were converted to gold (Au) nanowire networks through a lift-off pattern transfer process.[37,51,52] First, the PMMA domains of the block copolymer films were removed by exposure to UV light (254 nm and a dose of 1 J/cm^2) and development in a selective solvent (soaking in acetic acid for 30 min).[53] The film was then rinsed in cold DI water and dried. Subsequently, dry reactive ion etching was performed for 20 s in a PlasmaTherm 540 operating at 5.0 sccm O_2, 150 mTorr, and a power of 40 W. This process removes leftover PMMA and etches away the underlying brush layer from the substrate, thus

exposing the oxide substrate and leaving the PS template. Finally, 2 nm of a chrome (Cr) adhesion layer followed by 15 nm of Au was evaporated at ~1 Å/s using a CVC 3-boat thermal evaporator and without venting the chamber between metals. Networks of Au nanowires were then generated across the substrate by lifting-off the PS template by sonicating overnight in toluene.

The Au nanowire networks on oxide substrates were confined to micrometer-scale areas through conventional photolithographic processes. Briefly, the substrates were coated with NR9-1000P negative-tone photoresist, exposed through a Cr mask in a Suss MJB3 mask aligner (Hg lamp, 11 s exposure), and developed in RD-6 for 14 s. The metal nanowires in the regions uncovered by photoresist were then removed through wet chemical etching, with Transene TFA and TFN etchants being used for the Au and Cr metals, respectively. Photoresist was then stripped from the substrate by a short sonication in acetone. Contacts for electrical characterization were subsequently added using a lift-off process with the same photoresist and exposure/development steps. Metal deposition (2 nm of Cr and 50 nm of Au) was performed *via* thermal evaporation in the CVC 3-boat system. Liftoff was performed *via* rinsing in acetone followed by a short 5 min sonication. Residual organic material was removed *via* O_2 plasma in a March Jupiter III RIE.

Characterization: Electron Microscopy and *IV* Measurements. Images of the metal nanowires, as well as of the block copolymer morphology and the nanostructures during the fabrication process, were obtained in a JEOL JSM-7401F scanning electron microscope. An accelerating voltage of 3 kV was used with a sample bias of 2 kV. SEM images of the block copolymer and nanowire structure were analyzed after filtering to enhance domain contrast and equalize domain width, as detailed in ref 26. Continuous pixel areas were assigned a numerical designation and colorized for visual inspection. The largest PMMA or nanowire network in the image area is assigned a blue color.

Electrical transport in the nanowire networks was characterized by collecting current−voltage (*IV*) curves on a Bausch and Lomb probe station using an HP 4142B DC source/monitor. Voltage was swept between −100 and +100 mV and current was measured. Approximately 100 contacts were measured for each channel length and width. All contacts showed a linear ohmic response unless they were found to be disconnected, and conductance was determined as the slope of a linear best fit to the *IV* data.

Monte Carlo Model of Percolation. A simple Monte Carlo model to describe two-dimensional bond percolation behavior in confined systems was programmed in MATLAB R2013a. The 2D bond model is based on a square lattice of size N by M in which connections or "bonds" between individual nodes in the white domain are tracked within a 2D matrix.[42] As a result of this definition, a set of black nodes also resides within the lattice of white nodes, as illustrated in Figure 3A. When a connection is defined to exist between two nodes in the white domain, correspondingly two nodes in the black domain must be disconnected. Periodic boundary conditions are assigned such that the left/right and top/bottom edges of the simulation box are connected.

Initially, nodes are neither defined as being connected nor disconnected, and the simulation begins by randomly assigning the status of each connection. White bonds connecting the nodes are filled to match a user-specified volume fraction of the white domain within the overall lattice (*i.e.*, with domain concentrations similar to those in the block copolymer systems). With this initial random network assigned, rules are applied to the system to more realistically reflect the network structure formed by the lamellar block copolymer morphology in thin films. The unique bonding rules defined here to better capture the structure of block copolymer lamellae include the following:

1. Nodes with four bonds are forbidden. The dislocation and disclination defects in lamellae that lead to branching are at maximum 3-fold connected.
2. Nodes with no bonds (*i.e.*, zero-fold-connected or unconnected nodes) are forbidden. Such nodes would represent nonalternating lamellae due to the definition of volume fraction.

White or black nodes in the initial network that violate these bonding rules are addressed by randomly selecting and moving bonds to or from the remainder of the network. The simulation proceeds until all of the bonding rules are satisfied and the overall bonding concentration matches that initially defined. Note that these bonding rules limit the accessible symmetric concentrations for the lamellar morphologies to range from $(1/3)(N \times M)$ to $(2/3)(N \times M)$.

This Monte Carlo model allows for the efficient simulation of large 2D random bond networks (up to $N \times M = 10\,000$ considered here) and the calculation of ensemble averages performed over thousands of distinct network topologies. The network connectivity and percolation in the confined systems were determined *via* translation of the network structure to black and white images like that presented in Figure 3A panel 4 and characterization by the Image Analysis Toolbox in MATLAB R2013a. Briefly, continuous networks in the white or black domain were extracted and assigned a numerical designation, without consideration of the periodic boundaries assigned to create the image. Percolation across the image area was then determined by the presence of the same network on both image boundaries. The continuous networks were also colorized for visual inspection of network continuity as done in the SEM images.

Calculation of Conductance and Current Maps. Conductance was calculated from SEM and simulated images *via* network analysis in MATLAB R2013a and electric circuit calculation in NGSpice 26.[40] Segments connecting between branch points were extracted from the image and assigned a physical length based on the scale bar in SEM images and on assumed nanowire dimensions for the modeled systems. In both cases the nanowires were assumed to be exactly 15 nm tall and 25 nm wide. The resistivity of gold was specified to be 6.5×10^{-8} Ω·m for similarly sized and deposited nanowires as measured by Durkan *et al.*[41] The resistance of each segment was then calculated and exported along with connectivity information to NGSpice. A 1 V DC source was assumed to connect the left and right image borders. NGSpice returns the voltage drop through each resistor in the network, and from this the total current and conductance of the network were determined. Current maps were generated by normalization of the current through each segment and colorization of the original image.

Conflict of Interest: The authors declare no competing financial interest.

Acknowledgment. This research was supported by the University of Colorado and the Colorado Nanofabrication Laboratory/Nanomaterials Characterization Facility through the National Science Foundation (Grant No. ECS-0335765). The authors thank Dr. Kostas Daoulas for useful discussions.

Supporting Information Available: Additional high-resolution SEM images and discussion, verification of the fidelity of the lift-off pattern transfer process, and discussion of nonlinearity of conductance in random resistor networks. This material is available free of charge *via* the Internet at http://pubs.acs.org.

REFERENCES AND NOTES

1. Bates, F. S.; Fredrickson, G. H. Block Copolymer Thermodynamics - Theory and Experiment. *Annu. Rev. Phys. Chem.* **1990**, *41*, 525–557.
2. Kim, S. O.; Solak, H. H.; Stoykovich, M. P. Epitaxial Self-Assembly of Block Copolymers on Lithographically Defined Nanopatterned Substrates. *Nature* **2003**, *424*, 411–414.
3. Park, M.; Harrison, C.; Chaikin, P. M.; Register, R. A.; Adamson, D. H. Block Copolymer Lithography: Periodic Arrays of Similar to 10^{11} Holes in 1 Square Centimeter. *Science* **1997**, *276*, 1401–1404.
4. Park, C.; Yoon, J.; Thomas, E. Enabling Nanotechnology with Self Assembled Block Copolymer Patterns. *Polymer* **2003**, *44*, 6725–6760.
5. Hawker, C. J.; Russell, T. P. Block Copolymer Lithography: Merging "Bottom-Up" with "Top-Down" Processes. *MRS Bull.* **2005**, *30*, 952–966.

6. Segalman, R. A. Patterning with Block Copolymer Thin Films. *Mater. Sci. Eng. R Rep.* **2005**, *48*, 191–226.
7. Schneider, Y.; Modestino, M. A.; McCulloch, B. L.; Hoarfrost, M. L.; Hess, R. W.; Segalman, R. A. Ionic Conduction in Nanostructured Membranes Based on Polymerized Protic Ionic Liquids. *Macromolecules* **2013**, *46*, 1543–1548.
8. Jackson, E. A.; Hillmyer, M. A. Nanoporous Membranes Derived from Block Copolymers: From Drug Delivery to Water Filtration. *ACS Nano* **2010**, *4*, 3548–3553.
9. Park, M. J.; Balsara, N. P. Anisotropic Proton Conduction in Aligned Block Copolymer Electrolyte Membranes at Equilibrium with Humid Air. *Macromolecules* **2010**, *43*, 292–298.
10. Young, W.-S.; Epps, T. H., III. Ionic Conductivities of Block Copolymer Electrolytes with Various Conducting Pathways: Sample Preparation and Processing Considerations. *Macromolecules* **2012**, *45*, 4689–4697.
11. Wanakule, N. S.; Panday, A.; Mullin, S. A.; Gann, E.; Hexemer, A.; Balsara, N. P. Ionic Conductivity of Block Copolymer Electrolytes in the Vicinity of Order−Disorder and Order−Order Transitions. *Macromolecules* **2009**, *42*, 5642–5651.
12. Crossland, E. J. W.; Kamperman, M.; Nedelcu, M.; Ducati, C.; Wiesner, U.; Smilgies, D.-M.; Toombes, G. E. S.; Hillmyer, M. A.; Ludwigs, S.; Steiner, U.; *et al*. A Bicontinuous Double Gyroid Hybrid Solar Cell. *Nano Lett.* **2009**, *9*, 2807–2812.
13. Coakley, K. M.; Liu, Y.; McGehee, M. D.; Frindell, K. L.; Stucky, G. D. Infiltrating Semiconducting Polymers into Self-Assembled Mesoporous Titania Films for Photovoltaic Applications. *Adv. Funct. Mater.* **2003**, *13*, 301–306.
14. Rubatat, L.; Li, C.; Dietsch, H.; Nykänen, A.; Ruokolainen, J.; Mezzenga, R. Structure−Properties Relationship in Proton Conductive Sulfonated Polystyrene−Polymethyl Methacrylate Block Copolymers (sPS−PMMA). *Macromolecules* **2008**, *41*, 8130–8137.
15. Panday, A.; Mullin, S.; Gomez, E. D.; Wanakule, N.; Chen, V. L.; Hexemer, A.; Pople, J.; Balsara, N. P. Effect of Molecular Weight and Salt Concentration on Conductivity of Block Copolymer Electrolytes. *Macromolecules* **2009**, *42*, 4632–4637.
16. Okamoto, K.; Butsuen, A.; Tsuru, S.; Nishioka, S. Pervaporation of Water-Ethanol Mixtures through Poly-Dimethylsiloxane Block-Copolymer Membranes. *Polym. J.* **1987**, *19*, 747–756.
17. Zhou, M.; Nemade, P. R.; Lu, X.; Zeng, X.; Hatakeyama, E. S.; Noble, R. D.; Gin, D. L. New Type of Membrane Material for Water Desalination Based on a Cross-Linked Bicontinuous Cubic Lyotropic Liquid Crystal Assembly. *J. Am. Chem. Soc.* **2007**, *129*, 9574–9575.
18. Kim, B. J.; Fredrickson, G. H.; Hawker, C. J.; Kramer, E. J. Nanoparticle Surfactants as a Route to Bicontinuous Block Copolymer Morphologies. *Langmuir* **2007**, *23*, 7804–7809.
19. Bates, F. S. Network Phases in Block Copolymer Melts. *MRS Bull.* **2005**, *30*, 525–532.
20. Hashimoto, T.; Nishikawa, Y.; Tsutsumi, K. Identification of the "Voided Double-Gyroid-Channel": A New Morphology in Block Copolymers. *Macromolecules* **2007**, *40*, 1066–1072.
21. Majewski, P. W.; Osuji, C. O. Controlled Alignment of Lamellar Lyotropic Mesophases by Rotation in a Magnetic Field. *Langmuir* **2010**, *26*, 8737–8742.
22. Morkved, T. L.; Lu, M.; Urbas, A. M.; Ehrichs, E. E.; Jaeger, H. M.; Mansky, P.; Russell, T. P. Local Control of Microdomain Orientation in Diblock Copolymer Thin Films with Electric Fields. *Science* **1996**, *273*, 931–933.
23. Angelescu, D. E.; Waller, J. H.; Adamson, D. H.; Deshpande, P.; Chou, S. Y.; Register, R. A.; Chaikin, P. M. Macroscopic Orientation of Block Copolymer Cylinders in Single-Layer Films by Shearing. *Adv. Mater.* **2004**, *16*, 1736–1740.
24. Mullin, S. A.; Teran, A. A.; Yuan, R.; Balsara, N. P. Effect of Thermal History on the Ionic Conductivity of Block Copolymer Electrolytes. *J. Polym. Sci., Part B: Polym. Phys.* **2013**, *51*, 927–934.
25. Rubatat, L.; Shi, Z.; Diat, O.; Holdcroft, S.; Frisken, B. J.; Fraser, S.; Uni, V.; Va, B. C.; Cell, F.; Inno, V.; *et al*. Structural Study of Proton-Conducting Fluorous Block Copolymer Membranes. *Macromolecules* **2006**, *39*, 720–730.
26. Campbell, I. P.; Lau, G. J.; Feaver, J. L.; Stoykovich, M. P. Network Connectivity and Long-Range Continuity of Lamellar Morphologies in Block Copolymer Thin Films. *Macromolecules* **2012**, *45*, 1587–1594.
27. Unpublished Results of Sheet Resistance Measurements Made over ~1 cm Distances on Au Nanowire Networks Templated by Block Copolymer Lamellae in Thin Films.
28. Sax, J.; Ottino, J. Influence of Morphology on the Transport Properties of Polystyrene/polybutadiene Blends. 1. Experimental Studies. *Polymer* **1985**, *26*, 1073–1080.
29. Sax, J.; Ottino, J. M. Modeling of Transport of Small Molecules in Polymer Blends: Application of Effective Medium Theory. *Polym. Eng. Sci.* **1983**, *23*, 165–176.
30. Kinning, D.; Thomas, E.; Ottino, J. Effect of Morphology on the Transport of Gases in Block Copolymers. *Macromolecules* **1987**, *20*, 1129–1133.
31. Majewski, P. W.; Gopinadhan, M.; Osuji, C. Understanding Anisotropic Transport in Self-Assembled Membranes and Maximizing Ionic Conductivity by Microstructure Alignment. *Soft Matter* **2013**, *9*, 7106–7116.
32. Majewski, P. W.; Gopinadhan, M.; Jang, W.-S.; Lutkenhaus, J. L.; Osuji, C. O. Anisotropic Ionic Conductivity in Block Copolymer Membranes by Magnetic Field Alignment. *J. Am. Chem. Soc.* **2010**, *132*, 17516–17522.
33. Park, H. H. B.; Ha, S. Y. S.; Lee, Y. Y. M. Percolation Behavior of Gas Permeability in Rigid-Flexible Block Copolymer Membranes. *J. Membr. Sci.* **2000**, *177*, 143–152.
34. Hoarfrost, M. L.; Segalman, R. A. Conductivity Scaling Relationships for Nanostructured Block Copolymer/Ionic Liquid Membranes. *ACS Macro Lett.* **2012**, *1*, 937–943.
35. Cheng, J.; Ross, C. A.; Chan, V. Z. H.; Thomas, E. L.; Lammertink, R. G. H.; Vancso, G. J. Formation of a Cobalt Magnetic Dot Array via Block Copolymer Lithography. *Adv. Mater.* **2001**, *13*, 1174–1178.
36. Black, C. T.; Guarini, K. W.; Milkove, K. R.; Baker, S. M.; Russell, T. P.; Tuominen, M. T. Integration of Self-Assembled Diblock Copolymers for Semiconductor Capacitor Fabrication. *Appl. Phys. Lett.* **2001**, *79*, 409–411.
37. He, C.; Stoykovich, M. P. Profile Control in Block Copolymer Nanostructures Using Bilayer Thin Films for Enhanced Pattern Transfer Processes. *Adv. Funct. Mater.* **2014**, *24*, 7078–7084.
38. Mansky, P.; Liu, Y.; Huang, E.; Russell, T. P.; Hawker, C. J. Controlling Polymer-Surface Interactions with Random Copolymer Brushes. *Science* **1997**, *275*, 1458–1460.
39. Huang, E.; Rockford, L.; Russell, T. P.; Hawker, C. J. Nanodomain Control in Copolymer Thin Films. *Nature* **1998**, *395*, 757–758.
40. http://ngspice.sourceforge.net/.
41. Durkan, C.; Welland, M. Size Effects in the Electrical Resistivity of Polycrystalline Nanowires. *Phys. Rev. B* **2000**, *61*, 14215–14218.
42. Feng, X.; Deng, Y.; Blöte, H. W. J. Percolation Transitions in Two Dimensions. *Phys. Rev. E* **2008**, *78*, 031136.
43. Campbell, I. P.; He, C.; Stoykovich, M. P. Topologically Distinct Lamellar Block Copolymer Morphologies Formed by Solvent and Thermal Annealing. *ACS Macro Lett.* **2013**, *2*, 918–923.
44. Matsen, M. W.; Bates, F. S. Conformationally Asymmetric Block Copolymers. *J. Polym. Sci., Part B: Polym. Phys.* **1997**, *35*, 945–952.
45. Matsen, M. The Standard Gaussian Model for Block Copolymer Melts. *J. Phys.: Condens. Matter* **2002**, *14*, R21−R47.
46. Chintapalli, M.; Chen, X. C.; Thelen, J. L.; Teran, A. A.; Wang, X.; Garetz, B. A.; Balsara, N. P. Effect of Grain Size on the Ionic Conductivity of a Block Copolymer Electrolyte. *Macromolecules* **2014**, *47*, 5424–5431.
47. Ryu, H. J.; Sun, J.; Avgeropoulos, A.; Bockstaller, M. R. Retardation of Grain Growth and Grain Boundary Pinning in Athermal Block Copolymer Blend Systems. *Macromolecules* **2014**, *47*, 1419–1427.
48. Campbell, I. P.; Hirokawa, S.; Stoykovich, M. P. Processing Approaches for the Defect Engineering of Lamellar-Forming

Block Copolymers in Thin Films. *Macromolecules* **2013**, *46*, 9599–9608.
49. Han, E.; Stuen, K. O.; La, Y.-H.; Nealey, P. F.; Gopalan, P. Effect of Composition of Substrate-Modifying Random Copolymers on the Orientation of Symmetric and Asymmetric Diblock Copolymer Domains. *Macromolecules* **2008**, *41*, 9090–9097.
50. Ham, S.; Shin, C.; Kim, E.; Ryu, D. Y.; Jeong, U.; Russell, T. P.; Hawker, C. J. Microdomain Orientation of PS- B -PMMA by Controlled Interfacial Interactions. *Macromolecules* **2008**, *41*, 6431–6437.
51. Gowrishankar, V.; Miller, N.; McGehee, M. D.; Misner, M. J.; Ryu, D. Y.; Russell, T. P.; Drockenmuller, E.; Hawker, C. J. Fabrication of Densely Packed, Well-Ordered, High-Aspect-Ratio Silicon Nanopillars over Large Areas Using Block Copolymer Lithography. *Thin Solid Films* **2006**, *513*, 289–294.
52. Xiao, S.; Yang, X.; Lee, K. Y.; ver der Veerdonk, R. J. M.; Kuo, D.; Russell, T. P. Aligned Nanowires and Nanodots by Directed Block Copolymer Assembly. *Nanotechnology* **2011**, *22*, 305302.
53. Thurn-Albrecht, T.; Steiner, R.; DeRouchey, J.; Stafford, C. M.; Huang, E.; Bal, M.; Tuominen, M.; Hawker, C. J.; Russell, T. P. Nanoscopic Templates from Oriented Block Copolymer Films. *Adv. Mater.* **2000**, *12*, 787–791.